JMEPEG (2011) 20:276–282
DOI: 10.1007/s11665-010-9662-9

1059-9495/$19.00

XRD and SEM Investigation of Swift Heavy Ion-Irradiated Polyvinylidene Fluoride Thin Films

Dinesh Singh Rana, D.K. Chaturvedi, and J.K. Quamara

(Submitted March 26, 2009; in revised form January 21, 2010)

Polyvinylidene fluoride (PVDF) films of different thicknesses are irradiated with 100 meV Ag-ion and 75 meV Oxygen-ion beams at different fluences to study the effects of swift heavy ion (SHI) irradiation in PVDF. The change in physical, chemical, and surface morphological properties of irradiated films are investigated using x-ray diffraction, Field emission scanning electron microscopy (FESEM), and energy dispersive analysis by x-ray (EDAX) techniques by taking unirradiated (pristine) films as reference. The diffraction pattern shows that PVDF polymer is in semi-crystalline form and possesses crystalline α-, β-, and γ-phases. A decrease in the crystallinity and crystallite size has been observed when PVDF is irradiated with 100 meV Ag-, and also Oxygen ions at a higher fluence of 5.675×10^{12} ions/cm^2. However, an increase in crystallinity and decrease in crystallite size are observed when PVDF is irradiated with oxygen-ion beam at lower fluence 5.625×10^{11} ions/cm^2. The structural parameters such as degree of crystallinity, crystallite size, microstrain, and dislocation density have also been estimated. EDAX result shows that the chemical composition of PVDF is invariant under SHI irradiation, which is in agreement with our earlier results of FTIR. FESEM analysis shows granular microstructure with small porosity on SHI irradiation.

Keywords SHI, PVDF, FWHM, XRD, FESEM, EDAX

1. Introduction

Polyvinylidene fluoride (PVDF) has acquired immense importance in scientific and technological research because of its excellent mechanical, pyroelectric, ferroelectric, piezoelectric properties, and exceptional biocompatibility. PVDF is a semicrystalline polymer in which each monomer unit (CH_2-CF_2) has two dipole moments, one due to CF_2 and the other due to CH_2. It exhibits a variety of molecular conformations and crystalline phases such as α, β, γ, δ, and ε (Ref 1-3). The α-phase comprises helical structure whereas β-phase possesses all-trans planar zigzag conformation with dipole moments perpendicular to the chain axis, and the γ-phase with a structure intermediate to the helical α- and zigzag β-phases (Ref 4). The β-phase and sometimes the γ-phase can undergo reversible changes in polarization to create high piezoelectric and pyroelectric activity, which make PVDF as a very useful material in electronic activity (Ref 5) such as electromechanical, electro-acoustic transducers, and actuators. The exceptional biocompatibility of PVDF film is used in the development of skin transducer, implantable medical devices, and micro actuators (Ref 6).

The light weight and chemical resistance of PVDF polymers promote their use for the development of microsensors and actuators for space applications. However, in space, the performance of sensors and actuators may be affected due to the strong interaction of ultraviolet, γ-rays, x-rays, energetic ions, and atomic oxygen exposure with the sensor material. The interaction of these radiations with medium may change the physical, chemical, optical, structural, and morphological properties of PVDF films. The behavior of PVDF under bombardment of various kinds of radiation (Ref 7-15) has been studied before. These studies reveal the enhancement in electrical conductivity and change in crystallinity of PVDF (Ref 11). The decrease in crystallinity has been reported under low-energy ion implantation (Ref 11, 14) whereas an increase in crystallinity has been reported under electron and γ-ray irradiations (Ref 12, 15, 16). The crystallinity plays a crucial role in piezoelectric, mechanical, optical, electrical, and even thermal properties of polymers (Ref 11).

Swift heavy ion irradiation is a relatively new technique for modification of material properties. In an earlier article (Ref 17), we investigated SHI irradiation-induced changes in chemical and optical properties of PVDF films by comparing the FTIR and UV-Visible spectra of pristine and SHI-irradiated samples. The FTIR results show no significant formation of intermediate chemically distinct material on SHI irradiation. The UV-Visible absorption spectroscopy reveals hyperchromic, bathochromic, and hypsochromic shifts attributed to the formation of new defect sites. These studies are not able to detect the changes in the surface properties and crystalline structure. In this article, we investigate the physical, structural, chemical, and morphological changes in PVDF films due to SHI irradiation through the x-ray diffraction (XRD), field emission scanning electron microscopy (FESEM), and energy dispersive analysis by x-ray (EDAX) techniques. The transmission electron microscopy (TEM) and electron Scanning microscopy (SEM) are mainly used to examine structure on the surface and inside the object (<100 nm). Augmenting the

Dinesh Singh Rana and **D.K. Chaturvedi**, Institute of Instrumentation Engineering, Kurukshetra University, Kurukshetra 136119, India; and **J.K. Quamara**, Department of Physics, National Institute of Technology, Kurukshetra 136119, India. Contact e-mails: dineshsrana24@rediffmail.com and dineshsrana@yahoomail.com.

TEM method with high-resolution FESEM provides the facility to examine the overall particle shape, surface topography, and the side, and termination (particle end) geometries. To the best of our knowledge, this is the first time a detailed and comprehensive FESEM morphological characterization method has been presented for supplementing TEM analyses.

2. Experimental Details

The PVDF used in this study was procured from DuPont (USA) in flat film forms of thicknesses 9 and 20 μm. The samples of size 1 sq. cm were irradiated with 100 meV Ag-ion at the fluence of 1.875×10^{11} ions/cm^2 and with 75 meV oxygen ion at fluences 5.625×10^{11} ions/cm^2 and 5.675×10^{12} ions/cm^2 using the PELLETRON facility at Inter University Accelerator Centre, New Delhi. The samples were homogeneously irradiated on both faces in bulk by SHIs. The pristine and SHI-exposed PVDF films of different thicknesses were later investigated by XRD, SEM, and EDAX techniques.

The XRD analysis of pristine and irradiated samples was done using Bruker AXS D8 Advance diffractometer with operating target voltage of 40 kV and current 30 mA. X-ray data were collected for angular position 2θ in the interval 10°-50° in steps of 0.05° in 3 s, using Bruker AXS D8 powder diffractometer with Cu Kα (λ = 1.5406 Å) radiation source at the room temperature. Surface morphology of pristine and irradiated films has been investigated through TEM/FESEM using Quanta 200FEG instrument system having resolution of 2 nm at accelerating voltage of 30 kV with magnification; 1,000,000×. The chemical compositional identification is done by EDAX using EDX-INCA 350 Energy System (Energy Dispersive X-Ray System for SEM) attached to Quanta 200FEG instrument system.

3. Results and Discussion

3.1 X-ray Diffraction analysis

X-ray diffraction technique has been utilized to detect changes in crystalline and amorphous regions along with the degree of crystallinity. It is used to measure crystal structure, grain size, texture, and/or residual stress of materials through interaction of x-ray beams with samples. As x-rays are predominantly diffracted by electron density, analysis of the diffraction angles can be used to produce an electron density map of a given crystal or crystalline structure. The polycrystallinity of the pristine and the irradiated PVDF films are investigated using XRD analysis.

3.1.1 Pristine and Swift Heavy Ion-Irradiated PVDF. The XRD spectra of pristine PVDF films of different thicknesses are shown in Fig. 1(a) (for 9 μm) and (b) (for 20 μm). The diffraction patterns clearly indicate that the PVDF is semicrystalline in nature due to the folding and stacking of the PVDF polymer chains. The peak positions show crystalline α-, β-, and γ- phases and a broad background due to the scattering from amorphous regions of the polymer. The diffractogram is independent of the film thicknesses. The XRD data, i.e., angular positions (2θ), peak intensity (*I*), and lattice spacing (*d*) corresponding to α-, β-, γ-phases for pristine and ion-irradiated films of thickness 9 μm are given in Table 1 and for 20 μm films in Table 2. The pristine data are in conformity with those of other authors (Ref 11, 12, 14, 18, 19).

In order to investigate radiation-induced changes, we show in Fig. 2(a) and (b) the respective XRD spectra of 9- and 20-μm PVDF films irradiated with 100 meV Ag-ion at fluence 1.875×10^{11} ions/cm^2. The XRD data corresponding to crystalline α-, β-, and γ- phases in respect of 9- and 20-μm films are given in Table 1 and 2, respectively, along with pristine data. From the tables, we observe that on irradiation, the diffraction peaks corresponding to crystalline α-phase in 9-μm film get converted into the two closely spaced peaks at 2θ = 17.77°, and 18.63° with equal full width at half maxima (FWHM), whereas in 20-μm film only a broader peak at angular position 2θ = 17.79° is observed. We also observe sharp and well-defined diffraction peaks corresponding to the crystalline β- (110/200) phase and a broader peak corresponding to γ-phase.

Table 1 XRD data of 9 μm PVDF film before and after Ag-ion (fluence: 1.875×10^{11} ions/cm^2) irradiation

	Pristine film			Irradiated film		
Phase	**2θ**	***I***	***d*, Å**	**2θ**	***I***	***d*, Å**
α	17.77	2836	4.987	17.77	2402	4.986
				18.64	2296	4.756
β	20.08	3078	4.417	20.15	2359	4.402
γ	36.14	982	2.482	35.94	825	2.496

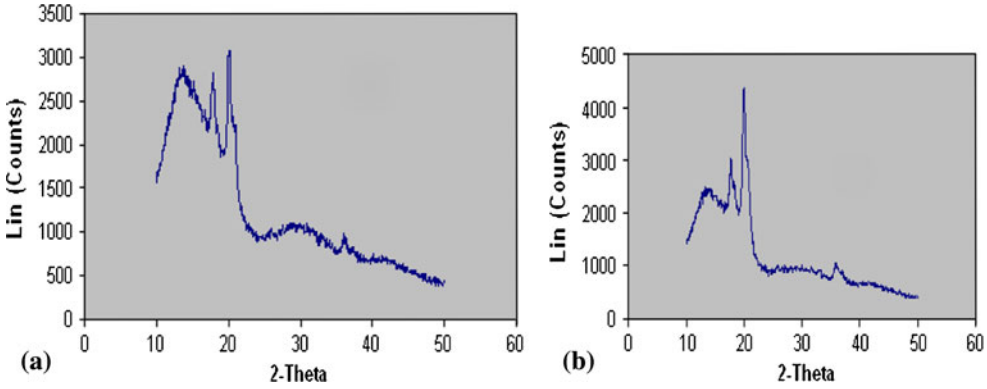

Fig. 1 XRD spectra of pristine PVDF films of thicknesses: (a) 9 μm and (b) 20 μm

Table 2 XRD data of 20 μm PVDF film before and after SHI irradiations

	Pristine			Irradiated 100 meV Ag-ion, 1.875×10^{11} ions/cm^2			Irradiated 75 meV oxygen-ion, 5.625×10^{11} ions/cm^2			Irradiated 75 meV oxygen-ion, 5.675×10^{12} ions/cm^2		
Phase	**2θ**	***I***	***d*, Å**	**2θ**	***I***	***d*, Å**	**2θ**	***I***	***d*, Å**	**2θ**	***I***	***d*, Å**
α	17.714	3015	5.002	17.79	2249	4.979	17.73	3060	4.990	17.76	2302	4.989
β	20.00	4351	4.449	20.15	2364	4.401	20.00	4442	4.446	20.05	2675	4.429
γ	35.92	1068	2.497	36.10	847	2.485	35.88	1085	2.500	35.94	893	2.496

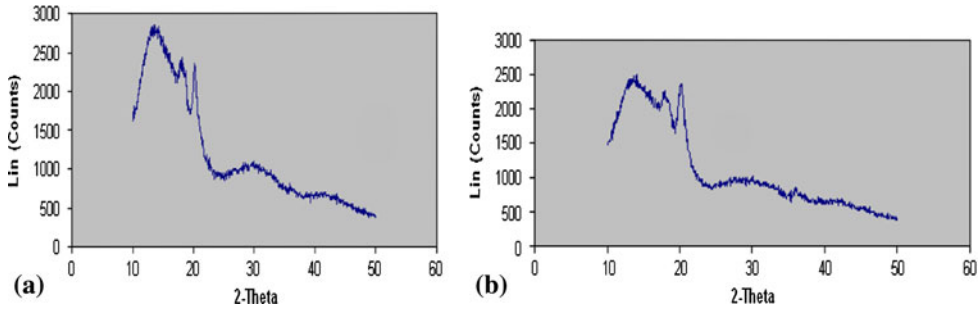

Fig. 2 XRD spectra of 100 meV Ag-ion (fluence: 1.875×10^{11} ions/cm^2)-irradiated PVDF films of thicknesses: (a) 9 μm and (b) 20 μm

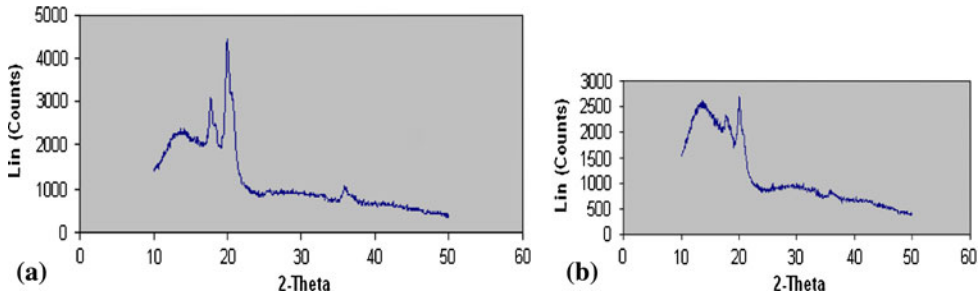

Fig. 3 XRD spectra of 20-μm PVDF film irradiated with 75 meV oxygen ion at fluences: (a) 5.625×10^{11} ions/cm^2 and (b) 5.675×10^{12} ions/cm^2

As compared to pristine films, the diffraction pattern of SHI-irradiated films (Fig. 1, 2, and Table 1, 2) not only show a decrease in intensity, but also the broadening of main diffraction peaks of crystalline α-, β-, and γ-phases. The decrease in peak intensity of diffraction peaks is usually related to the decrease in crystallinity, and the broadening of peaks is associated with the decrease in the mean crystallite size (Ref 11, 12, 15). The decrease in crystallinity on irradiation could be due to scission processes in the main chains of PVDF leading to the disruption in packing. The decrease in mean crystallite size is due to the formation of some small crystallites in the amorphous regions of films upon irradiation. The addition of these small crystallites with the original crystallites causes the mean size of the crystallite to decrease. We further observe that on irradiation, the angular positions of α- and β-phases get slightly shifted toward higher angles due to the decrease in lattice spacing d. This decrease in lattice spacing suggests that stress in film is compressive in nature.

Further, in order to investigate the irradiation-induced effect of different SHI and fluence on PVDF, we irradiated 20-μm PVDF film with 75 meV Oxygen-ion beam at fluences 5.625×10^{11} ions/cm^2 and 5.675×10^{12} ions/cm^2. The XRD spectra of film irradiated with these fluences are shown in Fig. 3(a) and (b), respectively. The XRD data for α-, β-, and γ-phases are given in Table 2 along with those of pristine and Ag-ion-irradiated film. It is interesting to note that Oxygen-ion-irradiated film at lower fluence (5.625×10^{11} ions/cm^2) shows broadening and an increase in the intensity, whereas broadening but decrease in intensity of main diffraction peaks are observed at higher fluence (5.675×10^{12} ions/cm^2). This shows that at higher fluence, amorphicity in PVDF increases due to scission processes, while at lower fluence, the crystallinity gets improved due to cross linking and realignment of molecular dipoles in PVDF, forming a hydrogen bond network into an ordered state of chain molecules in the crystalline regions and create volume elements as crystallites. These observations are in line with our estimation of degree of crystallinity to be presented in next section (Table 3).

From Table 2, it can also be observed that for similar fluence ($\sim 10^{11}$ ions/cm^2) irradiation-induced effect for Ag-ions are more pronounced as compared with Oxygen ions because of different electronic linear energy transfers associated with SHI.

For example, using the SRIM-08 code (Ziegler 2008), the projected range of 100 meV Ag-ion is estimated as 25.55 μm, whereas for 75 meV Oxygen ion, it comes out to be 105.35 μm, which is much larger than the PVDF film thickness (20 μm).

3.1.2 Crystallinity, Crystallite Size, and Other Structural Parameters. The structural parameters such as degree (percentage) of crystallinity (K), mean crystallite size (D), microstrain (ε), and dislocation density (δ) can be estimated from the XRD patterns of pristine and SHI-irradiated samples. The percentage of crystallinity (K) can be calculated from x-ray diffractogram by using the relation:

$$K = \frac{K_c(A1 + A2)}{K_c(A1 + A2) + K_a(A3)} \times 100 = \frac{(A1 + A2)}{(A1 + A2) + \frac{K_a}{K_c}(A3)} \times 100 \quad \text{(Eq 1)}$$

where $A1$ and $A2$ are the areas of two crystalline peaks superimposed on a broad amorphous hump of area $A3$ as shown in Fig. 4. K_a and K_c are proportionality constants for amorphous and crystalline phases, respectively. If we assume that polymer is 50% crystalline and 50% amorphous, then K_a is equal to K_c. Equation 1 then becomes

$$K = \frac{\Omega_c}{\Omega_t} \times 100, \quad \text{(Eq 2)}$$

where Ω_c denotes the total crystalline area, and Ω_t denotes the total area under the diffractogram. The estimated value of K for pristine and irradiated films of thicknesses 9 and 20 μm are tabulated in Table 3. As mentioned earlier, the increase in broadening of diffraction peak is related to the mean crystallite size (D) which can be estimated from the diffraction ray line broadening through Scherrer equation

$$D = \frac{C\lambda}{W \cos\theta} \quad \text{(Eq 3)}$$

where C is a constant which depends on diffractometer setup, λ is the wavelength of monochromatic radiation, θ is the diffraction angle or Bragg angle, and W denotes FWHM. For our setup, C is 0.9 and λ is 1.5406 Å. The values of W and θ can be obtained from the diffraction pattern.

The microstrain (Є) and dislocation density (δ) have been calculated using the following relations:

$$\epsilon = \frac{1}{4} W \cos\theta \quad \text{(Eq 4)}$$

and

$$\delta = \frac{1}{D^2} \quad \text{(Eq 5)}$$

As an illustration, in Table 4, we report the values of estimated structural parameters in β-phase only for pristine and irradiated films of different thicknesses. We observe that the average crystallite size (D) decreases upon SHI irradiation, which is in line with our interpretation of XRD spectra in Section 3.1.2. The microstrain (Є) and dislocation density (δ) in PVDF films increase on SHI irradiation, and the increase is more for Ag-ion as compared to Oxygen ion. The maximum micro strain is observed for Ag-ion-irradiated film of 20-μm thickness.

Table 3 Crystallinity of PVDF films of different thicknesses before and after SHI irradiations

Sample	Film thickness	
	9 μm	20 μm
Pristine	48.3%	51.53%
Irradiated Ag-ion, 1.875×10^{11} ions/cm^2	44.53%	48.5%
Irradiated oxygen-ion, 5.625×10^{11} ions/cm^2	···	55.69%
Irradiated oxygen-ion, 5.675×10^{12} ions/cm^2	···	47.08%-

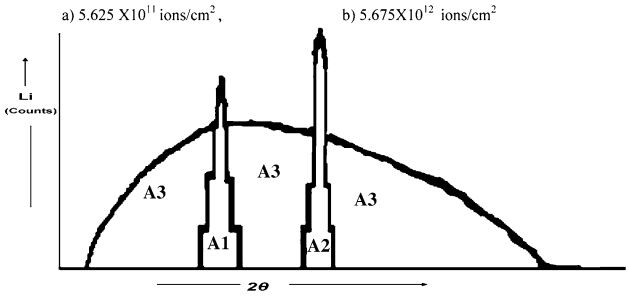

Fig. 4 XRD pattern with crystalline peaks and amorphous hump

3.2 Energy Dispersive Analysis by X-Ray

The EDAX microscopy is an indispensable tool for identification and measuring element composition on the surface of thin film samples of interest. The peak intensity in the energy dispersive x-ray (EDX) spectra represents a semi-quantitative relationship of the chemical elements present in the

Table 4 Structural parameters of PVDF film of different thicknesses in β-phase before and after SHI irradiation

Sample	Thickness											
	9 μm						20 μm					
	2θ, °	*W*, °	*W*, 10^{-3} rad	*D*, nm	Є, 10^{-3}	δ, 10^{15}	2θ, °	W, °	*W*, 10^{-3} rad	*D*, nm	Є, 10^{-3}	δ, 10^{15}
Pristine	20.08	0.45	7.850	17.93	1.94	3.11	20.00	0.45	7.850	17.93	1.94	3.11
Irradiated Ag-ion, 1.875×10^{11} ions/cm^2	20.15	0.50	8.720	16.13	2.15	3.84	20.15	0.70	12.220	12.08	3.22	6.85
Irradiated oxygen-ion, 5.625×10^{11} ions/cm^2							20.00	0.60	10.466	13.44	2.58	5.54
Irradiated oxygen-ion, 5.675×10^{12} ions/cm^2							20.05	0.55	9.594	14.67	2.36	4.7

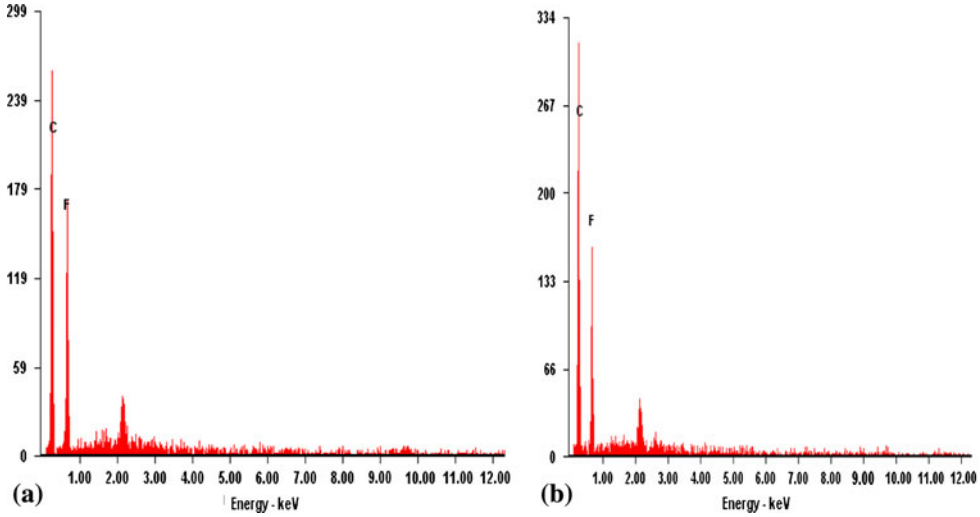

Fig. 5 EDX spectra of pristine PVDF of thicknesses: (a) 9 μm and (b) 20 μm

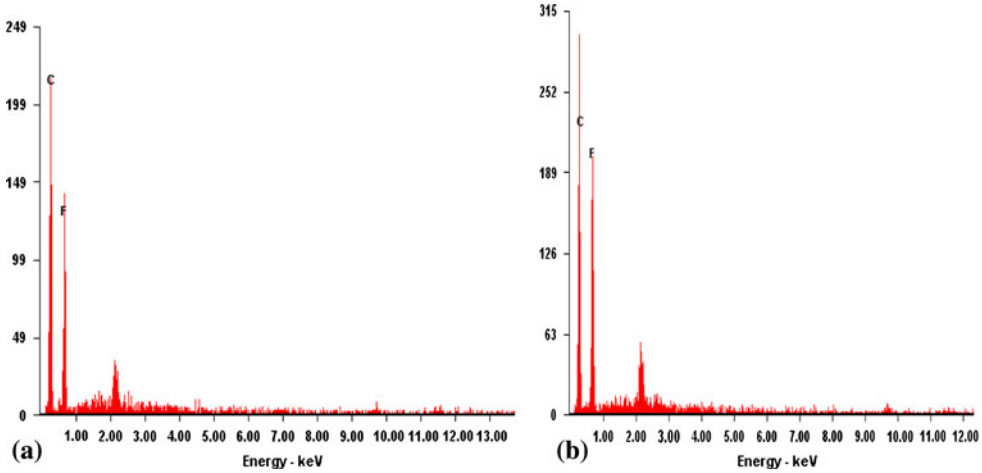

Fig. 6 EDX spectra of 100 meV Ag-ion (fluence: 1.875×10^{11} ions/cm^2) irradiated PVDF of thicknesses: (a) 9 μm and (b) 20 μm

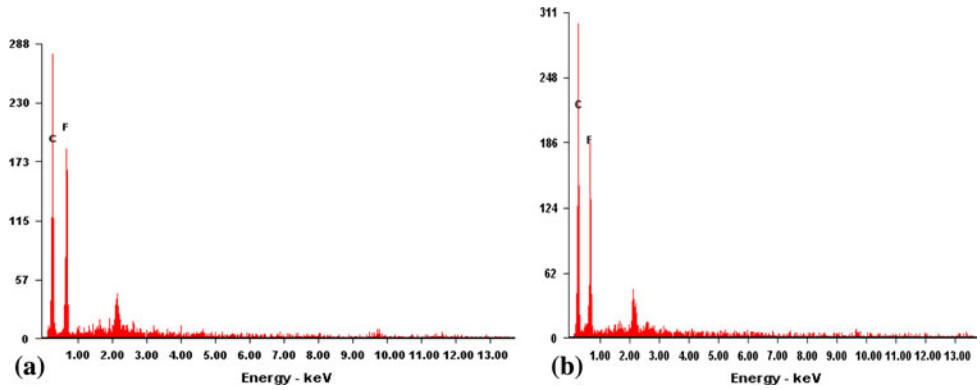

Fig. 7 EDX spectra of 20 μm PVDF film irradiated with 75 meV oxygen ion at fluences: (a) 5.625×10^{11} ions/cm^2 and (b) 5.675×10^{12} ions/cm^2

sample. EDAX microscopy cannot identify the chemical elements having atomic weight less than four, and hence we cannot find hydrogen in the EDX spectra. The EDX spectra of pristine and Ag-ion-irradiated PVDF films (for 9 and 20 μm) are illustrated in Fig. 5 and 6, respectively. The EDX spectra of 20 μm Oxygen-ion-irradiated film is shown in Fig. 7. All the spectra show only two peaks corresponding to main chemical elements, carbon and fluorine, originating from PVDF

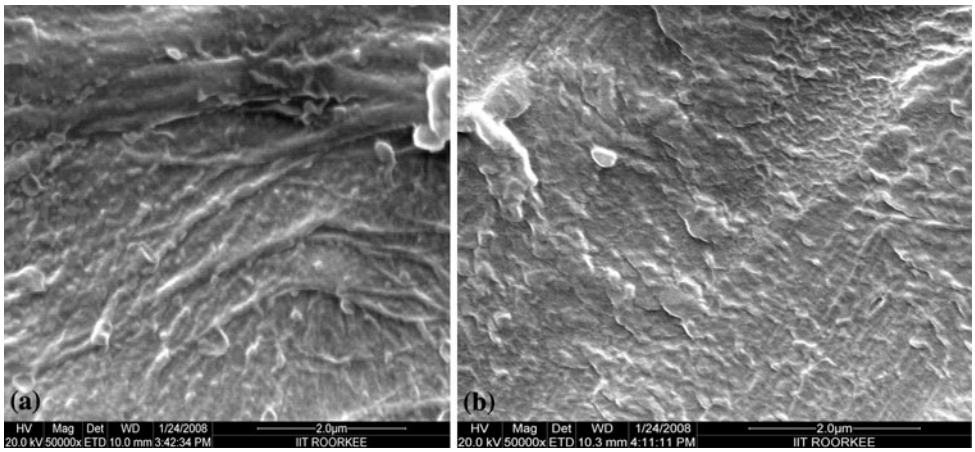

Fig. 8 ESEM micrographs of pristine PVDF films of thicknesses: (a) 9 μm and (b) 20 μm

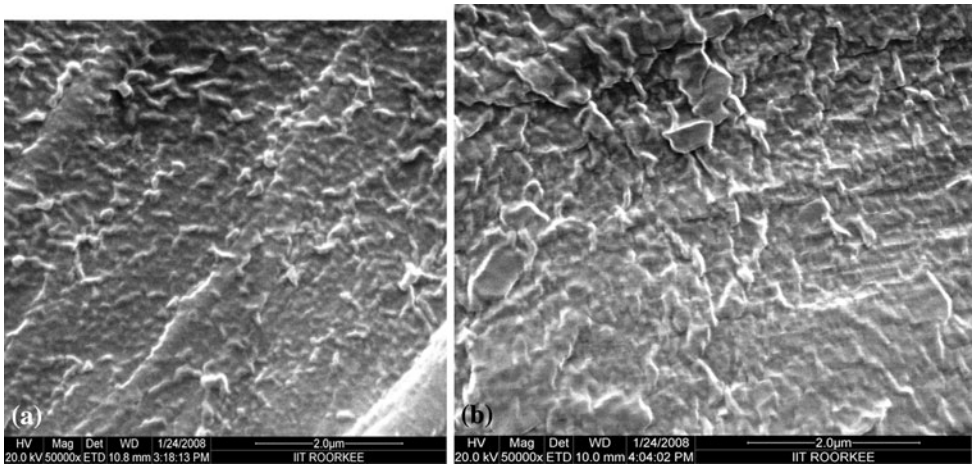

Fig. 9 ESEM micrographs of 100MeVAg-ion (fluence: 1.875×10^{11} ions/cm^2)-irradiated PVDF films of thicknesses: (a) 9 μm and (b) 20 μm

structure. We do not find any new peak in the EDX spectra of irradiated samples, which indicate that there is no formation of any new intermediate chemically distinct compound on irradiation. The appearance of third small peak in all the EDX spectra represents the presence of gold electrode deposited on the films for EDAX.

3.3 Field Emission Scanning Electron Microscopy

The FESEM is used for the investigation of topographic details on the surface and entire structure of the thin films. The emission scanning electron microscopic (ESEM) micrographs (at magnification of 50,000) of pristine and 100 meVAg-ion-irradiated PVDF films (9 and 20 μm) are shown in Fig. 8 and 9, respectively. The ESEM micrographs of 20 μm PVDF film irradiated with 75 meV oxygen-ion beam at fluences 5.625×10^{11} ions/cm^2 and 5.675×10^{12} ions/cm^2 are illustrated in Fig. 10(a) and (b), respectively.

Figure 8(a) and (b) clearly shows that pristine PVDF films possess long finger/fibers chain with sponge-like structures at the center in 9 μm film and a globular rock-like structure with small porous regions between the globes in 20 μm film. On irradiation with swift heavy Ag-ion, the surface morphology of both the films changes, and the samples show granular microstructure with increase in microporosity (Fig. 9a and b). The increase in porosity will enhance the ionic conduction through the irradiated films. The micrographs of 20 μm PVDF film irradiated with 75 meV oxygen-ion beam at different fluences reveal the increase in grain shape and size in granular microstructure with decrease in porosity. Figure 10(a) and (b) shows dark skin layer with distributed different-shaped grains of larger size, and the granular microstructure looks like dense globular rock-like structure. These results are in agreement with the estimation of crystallite size given in Table 4. The Ag-ion-irradiated films show higher porosity as compared with 75 meV oxygen ion at both the fluences. Thus, ionic conduction in Ag-ion-irradiated films will be higher than the film irradiated with oxygen ion.

4. Conclusions

We have investigated SHI irradiation-induced changes in PVDF thin films using XRD, EDAX, and FESEM techniques. The XRD spectra are used to estimate structural parameters such as degree of crystallinity, crystallite size, microstrain, and dislocation density of pristine and irradiated samples. The XRD

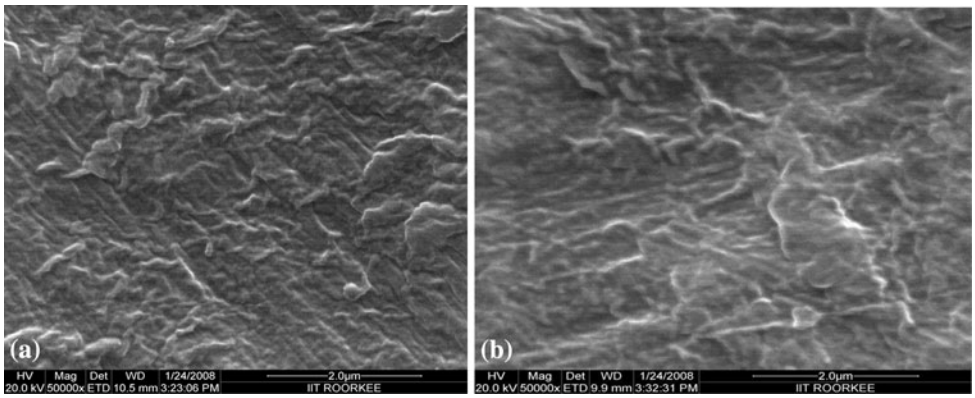

Fig. 10 ESEM micrographs of 20-μm PVDF film irradiated with 75 meV oxygen ion at fluences: (a) 5.625×10^{11} ions/cm^2 and (b) 5.675×10^{12} ions/cm^2

results show change in crystallinity and crystallite size upon irradiation, and the change depends on the type of SHI and fluence. The microstrain and dislocation density increase upon irradiation, and the maximum increases are observed for 20 μm PVDF film irradiated with Ag-ion beam. EDAX results show that the chemical composition of PVDF remains invariant under SHI irradiation, which is consistent with our earlier FTIR data (Ref 17). Therefore, PVDF may be used as a suitable material for sensors and actuators applications in radiation environment.

FESEM micrographs show granular and microporous surface morphology with adhesivity on SHI irradiation. The porosity is more with Ag-ion as compared to oxygen-ion-irradiated films. The porosity can be further enhanced through chemical etching process which will make PVDF film suitable for the use as separator in rechargeable batteries without sacrificing mechanical and thermal properties.

Acknowledgments

The authors are grateful to the Inter University Accelerator Centre, New Delhi, for providing the SHI irradiation facilities to carry out the research study, and to the Institute of Instrumentation Centre, IIT, Roorkee, for extending XRD and SEM facilities.

References

1. Q. Gao and J.I. Scheinbeim, Dipolar Intermolecular Interactions, Structural Development, and Electromechanical Properties in Ferroelectric Polymer Blends of Nylon-11 and Poly(vinylidene fluoride), *Macromolecules*, 2000, **33**(20), p 7564–7572
2. M. Benz and W.B. Euler, Determination of the Crystalline Phases of Poly(vinylidene fluoride) Under Different Preparation Conditions Using Differential Scanning Calorimetry and Infrared Spectroscopy, *J. Appl. Polym. Sci.*, 2003, **89**, p 1093–1100
3. N.J. Ramer, T. Marrone, K. Stiso et al., Structure and Vibrational Frequency Determination for α-Poly(vinylidene fluoride) Using Density-Functional Theory, *J. Polym.*, 2006, **47**, p 7160–7165
4. A. Nandi and L. Mandelkern, The Influence of Chain Structure on the Equilibrium Melting Temperature of Poly(vinylidene fluoride), *J. Polym.*, 2006, **29**, p 1287–1297
5. M.A. Doverspike and M.S. Conradi, Deuterium Magnetis Resonance Study of Orientation and Poling in Polyvinylidene Fluoride and Poly(vinylidene-fluoride-*co*-tetrafluoroethylene), *J. Appl. Phys.*, 1989, **65**, p 541–547
6. J. Ryu et al., Design and Fabrication of a Largely Deformable Sensorized Polymer Actuator, *Biosens. Bioelectr.*, 2005, **21**, p 822–826
7. E. Adem, J. Rickards, G. Burillo, and M. Avalos-Borja, Changes in Poly-Vinylidene Fluoride Produced by Electron Irradiation, *Radiat. Phys. chem.*, 1999, **54**, p 637–641
8. Z. Zhudi et al., Study on Gamma-Radiation Induced Lamellar Damage Mechanism of Poly(vinylidene fluoride), *Radiat. Phys. Chem.*, 1993, **41**, p 467–470
9. N. Betz, M.A. Le Mole, E. Balanzat, J.M. Ramillon, J. Lamotte et al., A FTIR Study of PVDF Irradiated by Means of Swift Heavy Ions, *J. Polym. Sci.*, 1994, **32**, p 1493–1502
10. Y. Komaki, N. Ishikawa, N. Morishita et al., Radicals in Heavy Ions Irradiated Polyvinylidene Fluoride, *Radiat. Measure.*, 1996, **26**, p 123–129
11. L. Calcagno, P. Musumeci, R. Percolla, and G. Foti, Changes in the Physical and Chemical Properties of PVDF Irradiated by 4 MeV Protons, *Nucl. Instr. Method Phys. Res.*, 1994, **B91**, p 461–464
12. K.D. Pae, S.K. Bhateja et al., Increase in Crystallinity in Poly(vinylidene fluoride) by Electron Beam Radiation, *J. Polym. Sci. B Polym. Phys.*, 1987, **25**, p 717–726
13. Z.X. Zhen, Long-Lived Fluoropolymeric Radicals in Irradiated Fluoropolymer Powders at Room Temperature, *Radiat. Phys. Chem.*, 1990, **35**, p 194–198
14. M.A. Said, C.M. Balik, and J.D. Carlson, High-Energy Ion Implantation of Polymers: Poly(vinylidene fluoride), *Polym. Sci. B Polym. Phys.*, 1988, **26**, p 1457
15. Y. Rosenberg, A. Sregmann, M. Narkis, and S. Shkolnik, Low Dose γ-Irradiation of Some Fluoropolymers: Effect of Polymer Chemical Structure, *J. Appl. Polym. Sci.*, 1992, **45**, p 783–795
16. Y.M. Lim, Y.M. Lee et al., Effect of Electron Beam Irradiation on Poly(vinylidene fluride) Films at the Melting Temperature, *J. Ind. Eng. Chem.*, 2006, **12**(4), p 589–593
17. D.S. Rana, D.K. Chaturvedi, and J.K. Quamara, Morphology, Crystalline Structure, and Chemical Properties of 100MeV Ag-ion Beam Irradiated Polyvinylidene Fluoride (PVDF) Thin Film, *J. Optoelectron. Adv. Mater.*, 2009, 11(5), p 705–712
18. B.E. Warren, *X-Ray Diffraction*, Dover Publication, New York, 1990
19. D.M. Esterly and B.J. Love, Phase Transformation to β-Poly(vinylidene fluoride) by Milling, *J. Polym. Sci. B Polym. Phys.*, 2004, **42**(1), p 91–97